Journal of Computational Physics, 232 (1), 2013, pp. 234–251.

Sheath Governing Equations in Computational Weakly-Ionized Plasmadynamics

Bernard Parent[*], Mikhail N. Shneider[†], and Sergey O. Macheret[‡]

To date, fluid models of plasma sheaths have consisted of the coupling of the electric field potential equation obtained through Gauss's law to the charged species conservation equations obtained through the drift-diffusion approximation. When discretized using finite-difference stencils, such a set of equations has been observed to be particularly stiff and to often require more than hundreds of thousands of iterations to reach convergence. A new approach at solving sheaths using a fluid model is here presented that reduces significantly the number of iterations to reach convergence while not sacrificing on the accuracy of the converged solution. The method proposed herein consists of rewriting the sheath governing equations such that the electric field is obtained from Ohm's law rather than from Gauss's law. To ensure that Gauss's law is satisfied, some source terms are added to the ion conservation equation. Several time-accurate and steady-state cases of dielectric sheaths, anode sheaths, and cathode sheaths (including glow and dark discharges) are considered. The proposed method is seen to yield the same converged solution as the conventional approach while exhibiting a reduction in computational effort varying between one-hundred-fold and ten-thousand-fold whenever the plasma includes both quasi-neutral regions and non-neutral sheaths.

1. Introduction

IN PLASMADYNAMICS, a "sheath" refers to a plasma region that is located adjacent to surface boundaries and that is significantly non-neutral. That is, a sheath always exhibits a substantial difference between its positive and negative charge densities. Several different types of sheaths are recognized, depending on the type of boundary material and also depending on the direction of the electric field near the surface. When the boundary is a dielectric, the electric field generally points towards the surface. In such a case, the plasma near the dielectric has an excess of positive charge, is a few Debye lengths thick, and is denoted as a "dielectric sheath". When the boundary is an electrode and the electric field points away from the surface, the plasma close to the electrode has an excess of negative charge and is denoted as an "anode sheath". When the boundary is an electrode and the electric field points towards the surface, the plasma close to the electrode has an excess of positive charge and is denoted as a "cathode sheath".

An accurate solution of the cathode sheath is generally crucial to predict correctly the current and electric field distribution through the rest of the plasma. This follows from the plasma near the cathode being characterized by an electron number density that is so low that the current in that region is mostly ionic rather than electronic. Because the ion mobility is substantially less than the electron mobility, it is not uncommon for the conductivity in the vicinity of the cathode to be less than one thousandth of the conductivity within the rest of the plasma. Such a low conductivity near the cathode results in a large voltage drop for a desired current, and this in turn leads to a large amount of power dissipated within the sheath in form of heat. Because of this, accurately modeling sheaths is generally deemed essential to assess adequately the performance of plasma-based devices such as MHD generators and accelerators [1, 2], or plasma actuators [3, 4, 5].

Because the sheath thickness is typically very small compared to the size of the plasma, its accurate resolution may necessitate a substantial refinement of the grid near the boundaries. To overcome this problem, the sheath and the plasma bulk can be solved through independent methods and "patched" to each other through some adequate boundary conditions [6, 7]. While

[*]Faculty Member, Dept. of Aerospace Engineering, Pusan National University, Busan 609-735, Korea, http://www.bernardparent.com.
[†]Senior Research Scientist, Dept. of Mechanical and Aerospace Engineering, Princeton University, Princeton, NJ 08544-5263, USA.
[‡]Senior Research Scientist, Dept. of Mechanical and Aerospace Engineering, Princeton University, Princeton, NJ 08544-5263, USA. Current address: Lockheed Martin Aeronautics Company, 1011 Lockheed Way, Palmdale, California 93599-0160.

the patching approach is advantaged by not requiring the sheath and the rest of the plasma to be solved in coupled form (hence providing substantial savings in computational effort) it is questionable how well it can model more complex situations where a strong coupling may occur, such as those involving motion of the neutrals and magnetic field effects.

To overcome the limitations of the patching method, a coupled solution of the plasma bulk and sheath is necessary. This can be accomplished through a kinetic simulation [8], a particle-in-cell simulation [9], or through a fluid model [10, 11, 12]. Also known as the "drift-diffusion" model, the fluid model is currently the method of choice in simulating sheaths that would occur within plasma aerodynamic applications (see for instance Refs. [13, 14, 15]). Indeed, when solving the relatively high density flows typical of plasma aerodynamics problems, the more detailed physical models associated with kinetic simulations or particle-in-cell simulations entail computing efforts that are beyond the capabilities of present computers.

To date, fluid models of plasma sheaths have consisted of the coupling of the electric field potential obtained through Gauss's law to the electron and ion conservation equations obtained through the drift-diffusion approximation. While such a strategy has had considerable success, it suffers from very slow convergence when solving plasmas that include quasi-neutral regions. When a quasi-neutral region forms within the plasma, the stiffness of the governing equations is such that typically one hundred thousand iterations or more are needed to reach steady-state. Such slow convergence has been observed not only for explicit relaxation schemes but also for fully-coupled implicit solvers. For this reason, quasi-neutral plasmas that do not include sheaths are typically solved by obtaining the electric field from Ohm's law rather than from Gauss's law. The stiffness of the governing equations is then relieved substantially and the computing effort can be reduced one-hundred-fold or even more. Such a strategy cannot be used for a plasma that includes non-neutral sheaths, however, because an electric field that is obtained from Ohm's law may not necessarily satisfy Gauss's law, and because the correct solution of Gauss's law is crucial to model the non-neutral regions of the plasma correctly.

It is here argued that the last statement is not necessarily correct. That is, it is not mandatory to obtain the electric field from Gauss's law to ensure that the latter is satisfied. As will be demonstrated in this paper, it is possible to use Ohm's law to obtain the electric field within the non-neutral sheath regions *while satisfying Gauss's law*. In so-doing, remarkable gains in computational efficiency are realized when solving plasmas that include both sheaths and quasi-neutral regions.

This paper does not constitute the first attempt at solving sheaths using Ohm's law. For instance, in Refs. [16, 17, 18], a thermionic cathode sheath is solved by determining the electric field from a form of Ohm's law. The method outlined in the latter references, however, does not ensure that Gauss's law is satisfied and is hence only applicable to thermionic sheaths, and not to cold cathode sheaths, dielectric sheaths, or anode sheaths. In contrast, we here propose a set of governing equations that is such that the electric field is determined from Ohm's law while ensuring that Gauss's law is satisfied. The novel set of governing equations proposed herein results in the same converged solution as the conventional set (in which the electric field is determined directly through Gauss's law) while yielding as much as a ten-thousand-fold reduction in computing effort. This is attributed to the proposed governing equations being considerably less stiff and hence permitting the use of significantly larger time steps when being integrated.

It is noted that a "stiff" system of equations here does not necessarily denote a system in which there is a large discrepancy between the eigenvalues or the physical time scales. Rather, we here adopt Lambert's definition of stiffness in the more general sense [19, page 220] with a slight modification to make it applicable to non-linear systems of equations:

> *Definition* If a numerical method, applied to a system with any initial conditions, is forced to use in a certain interval of integration a steplength which is excessively small in relation to the smoothness of the exact solution in that interval, then the system is said to be *stiff* in that interval.

When defined in this manner, stiffness is not an intrinsic property of the physical model: stiffness can originate from the disparity between the physical time scales, but can also originate from other attributes of the system of equations (see Chapter 6 in Ref. [19]). For instance, when a physical model involves several conservation laws dependent on each other, there is more than one way that the governing equations can be expressed, and the equations may exhibit more or less stiffness depending on how they are written, despite solving the same physical model and sharing the same physical time scales. Rewriting the governing equations differently while keeping the physical model the same was the strategy used to reduce the stiffness of the system associated with a quasi-neutral multicomponent plasma model in Ref. [20], with a currentless plasma model in Ref. [21], and with a two-fluid Euler-Poisson plasma model in Ref. [22]. The methods outlined in the latter references, however, can not be readily extended to the drift-diffusion model of sheaths. In this paper, we show that the stiffness of the system of equations associated with the drift-diffusion model of sheaths can also be alleviated substantially through a recast in different form, despite the recast set of equations solving the same physical model as the original set.

2. Physical Model

The physical model considered herein determines the electron, ion, and neutral properties through macroscopic-scale transport equations (*i.e.* the so-called drift-diffusion model). Such can accurately predict using the same set of differential equations both the non-neutral plasma sheaths and the quasi-neutral plasma bulk, including ambipolar diffusion and ambipolar drift phenomena. It is emphasized that the physical model presented in this section is commonly used to model sheaths taking place in weakly-ionized plasmas (plasmas with an ionization fraction less than 10^{-4}–10^{-3}). For instance, in Refs. [5, 10, 11, 12, 13, 14, 15], the same physical model as used herein (or a slight variant) is used to solve sheaths occurring in glow discharges, plasma aerodynamics, MHD generators, *etc.*

In a fluid model of plasmas, the conservation equation for each type of charged species can be expressed in general form as:

$$\frac{\partial N_k}{\partial t} + \frac{\partial}{\partial x}\left(N_k V_k\right) = W_k \tag{1}$$

where N_k is the number density, W_k represents the sources and sinks (*e.g.* due to ionization, recombination, attachment, and detachment), and V_k the charged species velocity including both drift and diffusion. Starting from the momentum equation of an unmagnetized plasma in which the neutrals are at rest, an expression for the charged species velocity can be derived:

$$V_k = s_k \mu_k E - \frac{\mu_k k_\mathrm{B} T_k}{|C_k| N_k}\frac{\partial N_k}{\partial x} \tag{2}$$

where s_k is the sign of the charge of the species under consideration (-1 for electrons, $+1$ for positive ions), C_k is the charge of the ion or electron under consideration (equal to $-e$ for the electrons and $+e$ for the singly-charged positive ions), E the electric field, T_k the temperature of the charged species, k_B the Boltzmann constant, and μ_k the mobility of the charged species.

By substituting the charged species velocity from Eq. (2) into Eq. (1), we obtain the ion and electron conservation equations:

$$\frac{\partial N_\mathrm{i}}{\partial t} + \frac{\partial}{\partial x}\left(\mu_\mathrm{i} N_\mathrm{i} E - D_\mathrm{i}\frac{\partial N_\mathrm{i}}{\partial x}\right) = W_\mathrm{i} \tag{3}$$

$$\frac{\partial N_\mathrm{e}}{\partial t} + \frac{\partial}{\partial x}\left(-\mu_\mathrm{e} N_\mathrm{e} E - D_\mathrm{e}\frac{\partial N_\mathrm{e}}{\partial x}\right) = W_\mathrm{e} \tag{4}$$

where we defined the ion and electron diffusion coefficients using the Einstein-Smoluchowski relationship:

$$D_\mathrm{i} \equiv \frac{\mu_\mathrm{i} k_\mathrm{B} T_\mathrm{i}}{e} \quad \text{and} \quad D_\mathrm{e} \equiv \frac{\mu_\mathrm{e} k_\mathrm{B} T_\mathrm{e}}{e} \tag{5}$$

To close the system of equations, it is necessary to find an expression for the electric field. This can be obtained from Gauss's law:

$$\frac{\partial E}{\partial x} = \frac{e}{\epsilon_0}(N_\mathrm{i} - N_\mathrm{e}) \tag{6}$$

with e the elementary charge and ϵ_0 the permittivity of free space.

In the physical model outlined above, the effects due to collisions between charged species, shear stresses, change of inertia, multiple ion species, acceleration of the bulk of the plasma, as well as the effects of diffusion due to temperature gradients, are ignored. This is not a source of concern as such effects are negligible in many weakly-ionized plasmas (see Ref. [23]). For example, the Coulomb collisions can be ignored in virtually all glow and non-equilibrium RF discharges where the ionization fraction is lower than 10^{-4}; one sort of ions often (albeit not always) dominates; the shear stresses can be demonstrated to be orders of magnitude lower than the collision forces, *etc.* Furthermore, the proposed method can readily be modified to include several of these effects. For instance, the collisions between charged species can be included simply by redefining the mobilities, leaving all other equations the same (see Chapter 2 in Ref. [24]). Similarly, the motion of the neutrals can be incorporated by adding the neutrals mass and momentum conservation equations. Nonetheless, we prefer not to do so in the present paper, because this would not impact appreciably the solution while increasing the complexity of the physical model unnecessarily. As well, we do not expect the addition of such effects to affect the gains in convergence acceleration obtained with the method proposed hereafter.

3. Conventional Sheath Governing Equations

The term "conventional governing equations" here denotes the set of partial differential equations that are generally used to solve the physical model outlined in the previous section. In the conventional set of governing equations, the electric field is determined from a form of the potential equation obtained from Gauss's law. This can be found starting from Eq. (6) and assuming that a potential ϕ exists such that $E = -\partial\phi/\partial x$:

$$\frac{\partial^2\phi}{\partial x^2} = -\frac{e}{\epsilon_0}(N_\mathrm{i} - N_\mathrm{e}) \tag{7}$$

The conventional governing equations hence consists of Eq. (7) and of the ion and electron conservation Eqs. (3)-(4). This can be expressed in general matrix form as:

$$R = Z\frac{\partial U}{\partial t} + \frac{\partial}{\partial x}(AU) - \frac{\partial}{\partial x}\left(K\frac{\partial U}{\partial x}\right) - S \tag{8}$$

with R the residual vector which we seek to minimize ($R \to 0$) and the U, S, A, K, Z matrices equal to:

$$U = \begin{bmatrix} N_\mathrm{i} \\ N_\mathrm{e} \\ \phi \end{bmatrix} \quad S = \begin{bmatrix} W_\mathrm{i} \\ W_\mathrm{e} \\ \frac{e}{\epsilon_0}(N_\mathrm{i} - N_\mathrm{e}) \end{bmatrix} \quad A = \begin{bmatrix} \mu_\mathrm{i}E & 0 & 0 \\ 0 & -\mu_\mathrm{e}E & 0 \\ 0 & 0 & 0 \end{bmatrix} \quad K = \begin{bmatrix} D_\mathrm{i} & 0 & 0 \\ 0 & D_\mathrm{e} & 0 \\ 0 & 0 & 1 \end{bmatrix} \quad Z = \begin{bmatrix} 1 & 0 & 0 \\ 0 & 1 & 0 \\ 0 & 0 & 0 \end{bmatrix} \tag{9}$$

The latter set of governing equations has been observed to be particularly stiff and difficult to integrate whenever a quasi-neutral region of substantial size appears within the solution. For such problems, numerical experiments indicate that the maximum time step that can be imposed on either the ion or electron conservation equation is limited by the CFL condition, even when using an implicit scheme. Because of the high electron velocity, a time-step bounded by the CFL condition effectively results in very slow convergence to steady-state, which is typically obtained after hundreds of thousands of iterations.

4. Proposed Sheath Governing Equations

To reduce the computational effort needed to solve plasmas that include both non-neutral and quasi-neutral regions, a new method is presented here. The method proposed consists of obtaining the electric field potential from a form of Ohm's law instead of Gauss's law. Then, to guarantee that Gauss's law is satisfied both in the neutral and quasi-neutral regions, some source terms are added to the ion conservation equation.

To yield a valid solution to the physical model presented in Section 2, the "Ohm's law" must be derived from the charged species conservation equations. This can be done by first subtracting the electron conservation equation (Eq. (4)) from the ion conservation equation (Eq. (3)):

$$\frac{\partial}{\partial t}(N_\mathrm{i} - N_\mathrm{e}) + \frac{\partial}{\partial x}\left((\mu_\mathrm{i}N_\mathrm{i} + \mu_\mathrm{e}N_\mathrm{e})E - D_\mathrm{i}\frac{\partial N_\mathrm{i}}{\partial x} + D_\mathrm{e}\frac{\partial N_\mathrm{e}}{\partial x}\right) = W_\mathrm{i} - W_\mathrm{e} \tag{10}$$

Because charge cannot be created or destroyed through the chemical reactions, it follows that the ion chemical source term cancels out the electron chemical source term ($W_\mathrm{i} - W_\mathrm{e} = 0$). Further, after multiplying all terms by the elementary charge e, we obtain:

$$\frac{\partial}{\partial t}e(N_\mathrm{i} - N_\mathrm{e}) + \frac{\partial J}{\partial x} = 0 \tag{11}$$

with the current density defined as:

$$J \equiv \sigma E - eD_\mathrm{i}\frac{\partial N_\mathrm{i}}{\partial x} + eD_\mathrm{e}\frac{\partial N_\mathrm{e}}{\partial x} \tag{12}$$

and with the conductivity defined as:

$$\sigma \equiv e(\mu_\mathrm{i}N_\mathrm{i} + \mu_\mathrm{e}N_\mathrm{e}) \tag{13}$$

Equation (12) is commonly referred to as Ohm's "law". It is pointed out that the form of Ohm's law presented in Eq. (12) and the conductivity presented in Eq. (13) are only applicable to the physical model outlined in Section 2. For a different physical

model, Ohm's law and the conductivity would take on different forms (see Ref. [23] for details). Further, should a potential ϕ exists such that $E = -\partial\phi/\partial x$, Eq. (11) becomes:

$$\frac{\partial}{\partial t} e(N_\mathrm{i} - N_\mathrm{e}) + \frac{\partial}{\partial x}\left(-\sigma\frac{\partial\phi}{\partial x} - eD_\mathrm{i}\frac{\partial N_\mathrm{i}}{\partial x} + eD_\mathrm{e}\frac{\partial N_\mathrm{e}}{\partial x}\right) = 0 \tag{14}$$

This completes our derivation of the potential equation based on Ohm's law. Because the latter is obtained solely from the ion and electron conservation equations, Eq. (14) is redundant. Indeed, the solution of Eq. (14) is guaranteed provided that the ion and electron conservation equations are solved. Alternately, the solution of the ion conservation equation is guaranteed provided that Eq. (14) and the electron conservation equation are solved. Because there are three unknowns (N_i, N_e, and E), it is hence necessary to find a third independent equation. This can be obtained by adding some source terms to the ion conservation equation to make sure that Gauss's law is enforced. For this purpose, recall the standard form of the ion conservation equation, Eq. (3):

$$\frac{\partial N_\mathrm{i}}{\partial t} - \frac{\partial}{\partial x}\left(D_\mathrm{i}\frac{\partial N_\mathrm{i}}{\partial x}\right) + \frac{\partial}{\partial x}\left(\mu_\mathrm{i} N_\mathrm{i} E\right) = W_\mathrm{i} \tag{15}$$

Split the last derivative on the LHS:

$$\frac{\partial N_\mathrm{i}}{\partial t} - \frac{\partial}{\partial x}\left(D_\mathrm{i}\frac{\partial N_\mathrm{i}}{\partial x}\right) + E\frac{\partial}{\partial x}\left(\mu_\mathrm{i} N_\mathrm{i}\right) + \mu_\mathrm{i} N_\mathrm{i}\frac{\partial E}{\partial x} = W_\mathrm{i} \tag{16}$$

But recall Gauss's law, Eq. (6), and substitute in the latter:

$$\frac{\partial N_\mathrm{i}}{\partial t} + E\frac{\partial}{\partial x}\left(\mu_\mathrm{i} N_\mathrm{i}\right) - \frac{\partial}{\partial x}\left(D_\mathrm{i}\frac{\partial N_\mathrm{i}}{\partial x}\right) = W_\mathrm{i} - \mu_\mathrm{i} N_\mathrm{i}\frac{e}{\epsilon_0}(N_\mathrm{i} - N_\mathrm{e}) \tag{17}$$

We now have 3 independent equations for three unknowns: (i) the newly-recast ion conservation equation including source terms to impose Gauss's law, Eq. (17), (ii) the electron conservation equation, Eq. (4), and (iii) the potential equation based on Ohm's law, Eq. (14). This set of equations can be written in general matrix form as follows:

$$R = Z\frac{\partial U}{\partial t} + \frac{\partial}{\partial x}(AU) + E\frac{\partial}{\partial x}(BU) - \frac{\partial}{\partial x}\left(K\frac{\partial U}{\partial x}\right) - S \tag{18}$$

with R the residual vector which we seek to minimize ($R \to 0$) and the U, S, Z, A, K, and B matrices equal to:

$$U = \begin{bmatrix} N_\mathrm{i} \\ N_\mathrm{e} \\ \phi \end{bmatrix} \quad S = \begin{bmatrix} W_\mathrm{i} - \mu_\mathrm{i} N_\mathrm{i}\frac{e}{\epsilon_0}(N_\mathrm{i} - N_\mathrm{e}) \\ W_\mathrm{e} \\ 0 \end{bmatrix} \quad Z = \begin{bmatrix} 1 & 0 & 0 \\ 0 & 1 & 0 \\ e & -e & 0 \end{bmatrix} \quad A = \begin{bmatrix} 0 & 0 & 0 \\ 0 & -\mu_\mathrm{e} E & 0 \\ 0 & 0 & 0 \end{bmatrix} \quad B = \begin{bmatrix} \mu_\mathrm{i} & 0 & 0 \\ 0 & 0 & 0 \\ 0 & 0 & 0 \end{bmatrix}$$
$$K = \begin{bmatrix} D_\mathrm{i} & 0 & 0 \\ 0 & D_\mathrm{e} & 0 \\ eD_\mathrm{i} & -eD_\mathrm{e} & \sigma \end{bmatrix} \tag{19}$$

Because the latter set of equations does not obtain the potential from Gauss's law, it is considerably less stiff and easier to integrate in the quasi-neutral limit than the standard set of sheath equations. The reasons for this will be discussed in Section 8 below. A similar strategy was employed in a previous paper by Crispel *et al.* [22] where the stiffness of the Euler-Poisson equations was alleviated by rewriting the set of equations such that the potential is not obtained from Gauss's law directly, but obtained from a different Poisson equation that is easier to integrate. However, the approach presented herein differs from the one outlined in Ref. [22] by being applicable to the drift-diffusion model rather than the Euler-Poisson model. Further, as will be shown below through numerous test cases, while such a recast of the equations relieves the stiffness of the system, it suffers from not exhibiting as high a resolution as the standard set of equations when solving sheaths (a higher resolution here implies a smaller numerical error on coarse meshes). This issue is now addressed by rewriting the electron conservation equation in "ambipolar form".

4.1. Ambipolar Form

The set of governing equations proposed in Eqs. (18)-(19) can be further improved by recasting the electron conservation equation in terms of drift and ambipolar diffusion terms. As was shown in Ref. [20], there is a computational advantage

in doing so: when written in ambipolar form, the charged species transport equations depend less strongly on the potential equation, and this leads to a beneficial reduction of the coupling between the potential and the electron and ion densities. To yield a computational advantage, however, the ambipolar diffusion terms must be written such that they do not depend on the electric field. Further, this needs to be accomplished while not altering the physical model shown above in Section 2. For these reasons, we follow Ref. [20] in which an approach is presented to obtain an exact solution to the ambipolar diffusion coefficient which is free of the electric field. This is in contrast to the ambipolar diffusion method proposed in Refs. [25, 26] which either yields an ambipolar diffusion coefficient function of the electric field, or alters the physical model through an approximate expression for the electric field found within the ambipolar diffusion terms.

Thus, following Ref. [20], we can derive the "ambipolar form" of the electron conservation equation from the physical model as follows. Let us first define E' as the component of the electric field that cancels out the component of the current originating from mass diffusion of the charged species (see the current components in Eq. (12)):

$$\sigma E' \equiv eD_\mathrm{i}\frac{\partial N_\mathrm{i}}{\partial x} - eD_\mathrm{e}\frac{\partial N_\mathrm{e}}{\partial x} \tag{20}$$

Isolate E':

$$E' = \frac{eD_\mathrm{i}}{\sigma}\frac{\partial N_\mathrm{i}}{\partial x} - \frac{eD_\mathrm{e}}{\sigma}\frac{\partial N_\mathrm{e}}{\partial x} \tag{21}$$

Recall the electron conservation equation, Eq. (4), and add and subtract E' to the electric field as follows:

$$\frac{\partial N_\mathrm{e}}{\partial t} + \frac{\partial}{\partial x}\left(-\mu_\mathrm{e}N_\mathrm{e}(E - E' + E') - D_\mathrm{e}\frac{\partial N_\mathrm{e}}{\partial x}\right) = W_\mathrm{e} \tag{22}$$

Then, let us substitute E' from Eq. (21) in the latter and regroup similar terms together:

$$\frac{\partial N_\mathrm{e}}{\partial t} + \frac{\partial}{\partial x}\left(-\mu_\mathrm{e}N_\mathrm{e}(E - E') - \frac{e}{\sigma}\mu_\mathrm{e}N_\mathrm{e}D_\mathrm{i}\frac{\partial N_\mathrm{i}}{\partial x} - \left(1 - \frac{e}{\sigma}\mu_\mathrm{e}N_\mathrm{e}\right)D_\mathrm{e}\frac{\partial N_\mathrm{e}}{\partial x}\right) = W_\mathrm{e} \tag{23}$$

But recall the definition of the conductivity from Eq. (13), $\sigma = e(\mu_\mathrm{i}N_\mathrm{i} + \mu_\mathrm{e}N_\mathrm{e})$. Then the last term on the LHS simplifies and the electron conservation equation becomes:

$$\frac{\partial N_\mathrm{e}}{\partial t} + \frac{\partial}{\partial x}\left(-\mu_\mathrm{e}N_\mathrm{e}(E - E') - \frac{e}{\sigma}\mu_\mathrm{e}N_\mathrm{e}D_\mathrm{i}\frac{\partial N_\mathrm{i}}{\partial x} - \frac{e}{\sigma}\mu_\mathrm{i}N_\mathrm{i}D_\mathrm{e}\frac{\partial N_\mathrm{e}}{\partial x}\right) = W_\mathrm{e} \tag{24}$$

The latter is the "ambipolar form" of the electron conservation equation. Indeed, noting that the ion mobility is much less than the electron mobility, it can be easily shown that the diffusion terms in Eq. (24) will collapse to the well-known ambipolar diffusion term for a three-component quasi-neutral plasma (see for instance Ref. [20]):

$$\frac{e}{\sigma}\mu_\mathrm{e}N_\mathrm{e}D_\mathrm{i}\frac{\partial N_\mathrm{i}}{\partial x} + \frac{e}{\sigma}\mu_\mathrm{i}N_\mathrm{i}D_\mathrm{e}\frac{\partial N_\mathrm{e}}{\partial x} \approx \left(1 + \frac{T_\mathrm{e}}{T_\mathrm{i}}\right)D_\mathrm{i}\frac{\partial N_\mathrm{e}}{\partial x} \quad \text{for } N_\mathrm{e} \approx N_\mathrm{i} \tag{25}$$

We emphasize that the newly derived ambipolar form of the electron conservation equation is obtained from the physical model without making any approximation. Because of this, whether the standard form Eq. (4) or the ambipolar form Eq. (24) of the electron conservation equation is solved, the solution obtained will be essentially the same provided enough grid points are used to minimize the numerical error. This is true when the plasma is quasi-neutral but also when the plasma exhibits considerable non-neutrality (such as within sheaths). Nevertheless, as will be shown below through some test cases, the ambipolar form does yield a much improved resolution on coarse meshes and thereby necessitates significantly fewer grid points to attain a grid-independent solution.

To summarize, the "ambipolar form" of the governing equations proposed herein consists of the potential equation found from Ohm's law Eq. (14), the recast ion conservation equation including Gauss's law Eq. (17), and the ambipolar form of the electron conservation equation Eq. (24). This set of equations can be written in general matrix form as follows:

$$R = Z\frac{\partial U}{\partial t} + \frac{\partial}{\partial x}(AU) + E\frac{\partial}{\partial x}(BU) - \frac{\partial}{\partial x}\left(K\frac{\partial U}{\partial x}\right) - S \tag{26}$$

with R the residual vector which we seek to minimize ($R \to 0$) and the U, S, Z, A, K, and B matrices equal to:

$$U = \begin{bmatrix} N_\mathrm{i} \\ N_\mathrm{e} \\ \phi \end{bmatrix} \quad S = \begin{bmatrix} W_\mathrm{i} - \mu_\mathrm{i} N_\mathrm{i} \frac{e}{\epsilon_0}(N_\mathrm{i} - N_\mathrm{e}) \\ W_\mathrm{e} \\ 0 \end{bmatrix} \quad Z = \begin{bmatrix} 1 & 0 & 0 \\ 0 & 1 & 0 \\ e & -e & 0 \end{bmatrix} \quad A = \begin{bmatrix} 0 & 0 & 0 \\ 0 & -\mu_\mathrm{e}(E - E') & 0 \\ 0 & 0 & 0 \end{bmatrix} \quad B = \begin{bmatrix} \mu_\mathrm{i} & 0 & 0 \\ 0 & 0 & 0 \\ 0 & 0 & 0 \end{bmatrix}$$
$$K = \begin{bmatrix} D_\mathrm{i} & 0 & 0 \\ \frac{e}{\sigma}\mu_\mathrm{e} N_\mathrm{e} D_\mathrm{i} & \frac{e}{\sigma}\mu_\mathrm{i} N_\mathrm{i} D_\mathrm{e} & 0 \\ e D_\mathrm{i} & -e D_\mathrm{e} & \sigma \end{bmatrix} \tag{27}$$

Through various numerical experiments performed in Section 8 below, the latter set of governing equations will be demonstrated to be considerably easier to integrate than the standard set despite solving the same physical model and hence yielding the same converged solution (provided that the mesh is refined sufficiently to minimize the numerical error). In fact, the improvement in convergence rate will be shown to be of one-hundred-fold or more whenever the plasma includes both non-neutral sheaths and quasi-neutral regions. It may be argued that there are other ways that the governing equations can be formulated while not altering the physical model. In principle, it is possible that a formulation can be discovered that is even more computationally efficient than the one outlined above. We wish to point out, however, that we did explore several other approaches: those proved to be either more difficult to integrate, or resulted in a less accurate solution on coarse meshes than the method proposed herein.

5. Discretization of the Governing Equations

Noting that the residual for the conventional set of sheath governing equations (see Eq. (8)) has the same form as the residual for the proposed sets of sheath governing equations (see Eq. (18) and (26)), we can express both sets of governing equations in discrete form as follows:

$$R_\Delta = Z\delta_t(U) + \delta_x(AU) + E\delta_x(BU) - \delta_x\left(K\delta_x(U)\right) - S \tag{28}$$

where R_Δ is the discretized residual which we seek to minimize, and where $\delta_x()$ and $\delta_t()$ are some discretization operators which vary depending on the term being discretized. The discrete temporal derivative term, the discrete convection terms, and the discrete diffusion term are given the following discretization stencils:

$$Z\delta_t(U) = Z_i\left(\frac{U_i - U_i^{t-\Delta t}}{\Delta t}\right) \tag{29}$$

$$\delta_x(AU) = \frac{(AU)_{i+1/2} - (AU)_{i-1/2}}{\Delta x} \tag{30}$$

$$E\delta_x(BU) = \left(\frac{E_{i-1/2} + |E_{i-1/2}|}{2}\right)\left(\frac{(BU)_i - (BU)_{i-1}}{\Delta x}\right) + \left(\frac{E_{i+1/2} - |E_{i+1/2}|}{2}\right)\left(\frac{(BU)_{i+1} - (BU)_i}{\Delta x}\right) \tag{31}$$

$$\delta_x\left(K\delta_x(U)\right) = \frac{(K_i + K_{i+1})(U_{i+1} - U_i) - (K_{i-1} + K_i)(U_i - U_{i-1})}{2\Delta x^2} \tag{32}$$

In the latter, i denotes the grid index along x, and $(t - \Delta t)$ refers to the properties at the previous time level.

In Eq. (30), the convective flux at the interface $(AU)_{i+1/2}$ is determined from a Steger-Warming scheme [27] turned second-order accurate through an upwinded Van-Leer TVD limiter [28]. In determining the flux at the interface through the Steger-Warming scheme, the stencil can be simplified considerably noting that the convective flux Jacobian A is a diagonal matrix; then, the left and right eigenvector matrices can be set to the identity matrix I, and the eigenvalue matrix set to the Jacobian matrix A.

In Eq. (31), the electric field at the interface is determined from the potential as follows:

$$E_{i+1/2} = -\frac{\phi_{i+1} - \phi_i}{\Delta x} \tag{33}$$

When the electric field at a specific node is required, it is determined from the arithmetic average of the electric fields at the adjacent interfaces except when computing the Townsend ionization source terms where it is obtained from the minmod of the electric fields on the adjacent interfaces:

$$E_i = \begin{cases} \mathrm{minmod}(E_{i-1/2},\ E_{i+1/2}) & \text{when computing chemical source terms} \\ \frac{1}{2}\left(E_{i-1/2} + E_{i+1/2}\right) & \text{otherwise} \end{cases} \tag{34}$$

with the minmod function returning the argument with the lowest magnitude if both arguments have the same sign, and returning zero otherwise.

All the discretization stencils shown above are monotonicity-preserving. That is, they will not introduce spurious oscillations in the solution even in the vicinity of large gradients. It is noted that the discrete terms $Z\delta_t U$ and $E\delta_x(BU)$ use first-order accurate stencils in contrast to the other terms which utilize second-order accurate stencils. First-order stencils are chosen for the terms $Z\delta_t U$ and $E\delta_x(BU)$ because it is not clear how these stencils can be extended to second-order accuracy while remaining monotonicity-preserving and because the monotonicity-preserving property is crucial in obtaining physically-meaningful results of sheaths. Indeed, as will be shown below within the test cases section, the electron and ion number densities can vary by several orders of magnitude within a few nodes when solving sheaths, and a scheme that is not monotonicity-preserving would likely induce spurious oscillations that may result in negative (and hence, aphysical) charge densities. Further, several grid convergence studies performed for steady-state problems will demonstrate that the use of a first-order stencil for the term $E\delta_x(BU)$ is not a particular source of concern when solving sheaths because most of the numerical error originates from the $\delta_x(AU)$ and $\delta_x(K\delta_x(U))$ terms which use second-order stencils.

6. Pseudotime Relaxation of the Discretized Equations

To attain a converged solution, the discrete residual outlined in Eq. (28) must be reduced to a small quantity at every node. This is here accomplished through the use of pseudotime relaxation combined with a block-implicit method. A block-implicit pseudotime relaxation strategy is chosen because it is the preferred relaxation technique in various compressible fluid dynamics and plasma aerodynamics codes (see NASA's OVERFLOW and CFL3D codes for instance or the recent papers in plasma aerodynamics). Therefore, the convergence gains reported herein are likely to be reproduced when the sheath equations in the existing codes are replaced by the sheath equations proposed in this paper.

Let us add for this purpose a pseudotime derivative to the discretization equation (*i.e.* Eq. (28)) and rewrite in delta form:

$$Y\Delta^n U + \Delta^n(Z\delta_t U) + \delta_x\Delta^n(AU) + \Delta^n(E\delta_x BU) - \delta_x\Delta^n\left(K\delta_x U\right) - \Delta^n S = -R^n_\Delta \tag{35}$$

In the latter, $\Delta^n() \equiv ()^{n+1} - ()^n$ with the superscript n denoting the pseudotime level. As well, Y is a diagonal matrix related to pseudotime relaxation:

$$Y = \begin{bmatrix} 1/(\Delta\tau)_{\mathrm{i}} & 0 & 0 \\ 0 & 1/(\Delta\tau)_{\mathrm{e}} & 0 \\ 0 & 0 & 1/(\Delta\tau)_\phi \end{bmatrix} \tag{36}$$

where $(\Delta\tau)_{\mathrm{i}}$, $(\Delta\tau)_{\mathrm{e}}$, and $(\Delta\tau)_\phi$ are the pseudotime steps for the ion conservation, electron conservation, and potential equations, respectively.

Consider a relaxation process such that the diffusion matrix K, the convective flux Jacobian A, the electric field E, and the matrices B, Y, and Z remain frozen from pseudotime level n to pseudotime level $n+1$. The relaxed discretization equation to solve at the ith node then takes the form:

$$\begin{aligned} &-\left(\frac{1}{\Delta x^2}K^n_{i-1/2} + \frac{|E^n_{i-1/2}| + E^n_{i-1/2}}{2\Delta x}B^n_{i-1} + \frac{1}{2\Delta x}|A|^n_{i-1} + \frac{1}{2\Delta x}A^n_{i-1}\right)\Delta^n U_{i-1} + \left(Y^n_i + \frac{1}{\Delta t}Z^n_i\right. \\ &\left.+\frac{1}{\Delta x^2}K^n_{i-1/2} + \frac{1}{\Delta x^2}K^n_{i+1/2} - M^n_i + \frac{|E^n_{i-1/2}| + E^n_{i-1/2} + |E^n_{i+1/2}| - E^n_{i+1/2}}{2\Delta x}B^n_i + \frac{1}{\Delta x}|A|^n_i\right)\Delta^n U_i \\ &-\left(\frac{1}{\Delta x^2}K^n_{i+1/2} + \frac{|E^n_{i+1/2}| - E^n_{i+1/2}}{2\Delta x}B^n_{i+1} + \frac{1}{2\Delta x}|A|^n_{i+1} - \frac{1}{2\Delta x}A^n_{i+1}\right)\Delta^n U_{i+1} = -(R^n_\Delta)_i \end{aligned} \tag{37}$$

In the latter, the matrix M corresponds to the source term Jacobian (*i.e.* $M \equiv \partial S/\partial U$) but excluding the linearization of the Townsend ionization terms. Excluding the Townsend ionization terms from the source term Jacobian results in a more stable relaxation hence permitting the use of higher pseudotime steps leading to faster convergence. Additionally, it is found that faster convergence is obtained by not including the second-order terms of the convection derivative $\delta_x AU$ on the LHS of Eq. (37). Not only would this require the inversion of a penta-diagonal matrix instead of a tri-diagonal matrix, but this would also often lead to some convergence hangs caused by the flux limiter.

In solving Eq. (37), the electron and ion conservation equations are advanced in pseudotime in coupled form through a block-TDMA (*i.e.* the tri-diagonal matrix algorithm is modified so that it inverts a matrix whose elements are 2×2 matrices). On the other hand, the potential equation is not integrated in coupled form with the charged species conservation equations,

but is rather relaxed through a scalar-TDMA once the ion and electron densities have been updated. One pseudotime iteration hence consists of first finding the residual of the charged species conservation equations through Eq. (28), then updating the electron and ion densities in coupled form using Eq. (37), then finding the residual of the potential equation through Eq. (28), and then updating the potential equation using Eq. (37). Such a relaxation strategy is here chosen because it corresponds to the one generally employed in plasma solvers in which the electric field is obtained from the potential equation (that is, the potential equation and the fluid flow equations are solved consecutively through separate methods).

The iteration process outlined above is repeated as long as the residual remains above a certain user-defined threshold. When the magnitude of the residual of all nodes becomes less than the user-defined threshold, the discretized equations are considered converged and the iteration process stopped. To improve the rate of convergence, the pseudotime step is allowed to vary within the computational domain (*i.e.* local pseudotime stepping). Through a trial-and-error approach, it is found that optimal convergence rates are attained when the ion, electron, and potential pseudotime steps at the ith node are set equal to:

$$(\Delta\tau)_{\mathrm{i}} = \mathrm{CFL} \times \frac{\Delta x}{a_{\mathrm{ref}} + \max(|v_{\mathrm{i}}|_{i-1/2},\ |v_{\mathrm{i}}|_{i+1/2})} \tag{38}$$

$$(\Delta\tau)_{\mathrm{e}} = \mathrm{CFL} \times \frac{\Delta x}{a_{\mathrm{ref}} + \sqrt{\mu_{\mathrm{i}}/\mu_{\mathrm{e}}} \times \max(|v_{\mathrm{e}}|_{i-1/2},\ |v_{\mathrm{e}}|_{i+1/2})} \tag{39}$$

$$(\Delta\tau)_{\phi} = \begin{cases} L_{\mathrm{c}} \times \Delta x & \text{for the potential equation based on Gauss's law} \\ L_{\mathrm{c}} \times \dfrac{\Delta x}{\max(\sigma_{i-1/2},\ \sigma_{i+1/2})} & \text{for the potential equation based on Ohm's law} \end{cases} \tag{40}$$

In the latter, the ion and electron "drift" velocities are defined as follows:

$$v_{\mathrm{i}} \equiv \mu_{\mathrm{i}}(E - E') \quad \text{and} \quad v_{\mathrm{e}} \equiv -\mu_{\mathrm{e}}(E - E') \tag{41}$$

In Eqs. (38)-(40), CFL is a non-dimensional user-defined parameter, a_{ref} is a reference sound speed typically set to 300 m/s, and L_{c} is a user-defined length scale. The latter user-defined parameters are constant throughout the computational domain for a given pseudotime level, but may be varied as a function of the iteration count to further improve the convergence rates. Details on how the parameters CFL and L_{c} are specified will be given for each test case in Section 8 below.

7. Boundary Conditions

At the interface between the plasma and a solid surface, the boundary conditions for the electron and ion number densities depend on the direction of the electric field. For this purpose, it is convenient to consider a coordinate η which is oriented perpendicular to the surface and which points away from the surface. Then, when the electric field vector points away from the surface, the boundary conditions take the form:

$$\frac{\partial(N_{\mathrm{e}}V_{\mathrm{e}})}{\partial x} = 0 \quad \text{and} \quad N_{\mathrm{i}} = 0 \quad \text{for } E_\eta > 0 \tag{42}$$

On the other hand, when the electric field vector points towards the surface, the boundary conditions are specified as proposed in Ref. [14]:

$$\frac{\partial(N_{\mathrm{i}}V_{\mathrm{i}})}{\partial x} = 0 \quad \text{and} \quad N_{\mathrm{e}} = \gamma N_{\mathrm{i}} \frac{\mu_{\mathrm{i}}}{\mu_{\mathrm{e}}} \quad \text{for } E_\eta < 0 \tag{43}$$

In the latter, γ is the secondary emission coefficient (*i.e.*, the ratio between the electron flux emanating from the surface and the ion flux impinging the surface), and E_η is the component of the electric field along the coordinate η. We note that Eq. (43) is intended to be applied on surfaces that do not reflect charged species, such as electrodes or dielectrics that absorb all incoming electrons and ions. Moreover, Eq. (43) can not be applied to surfaces for which thermionic emission is significant. The reader is referred to Ref. [29] for boundary conditions at a surface that reflects all incoming electrons and to Refs. [16, 17] for boundary conditions at the cathode including thermionic emission. Using the cathode boundary conditions outlined in the latter references has been verified not to alter significantly the convergence rates: when these boundary conditions are substituted to the ones shown in Eq. (43), the gains in convergence rates exhibited by the proposed method over the conventional approach remain essentially the same.

When using the set of governing equations proposed herein, imposing the anode boundary condition outlined in Eq. (42) can lead to some difficulties within the anode sheath (*i.e.*, the sheath in the vicinity of an electrode with the electric field pointing

away from the surface). The problem arises from the electron conservation equation and the electric field potential equation not depending significantly on the ion number density when the electron density largely exceeds the ion density, as is the case within anode sheaths close to the surface. Because of this, and because Gauss's law is enforced through the solution of the ion conservation equation, it follows that the distribution of the electron density at the anode sheath boundary may not obey Gauss's law. Put differently, because Gauss's law is enforced through some source terms added to the ion transport equation, and because these source terms scale with the ion density and hence vanish in flow regions where the ion density becomes zero (see Eq. (17)), Gauss's law may not be satisfied in flow regions where the ion density is zero, as is the case at the anode. For this reason, it is necessary to rewrite the boundary condition for the electron number density at the anode to ensure that Gauss's law is satisfied. This can be obtained starting from the definition of the current density, Eq. (12), substituting E' from Eq. (21) and σ from Eq. (13), and noting that N_i is zero at the anode. An expression is then obtained for the current at the anode:

$$J = e\mu_\mathrm{e} N_\mathrm{e}(E - E') \tag{44}$$

Take the derivative with respect to x of all terms, assuming constant μ_e:

$$\frac{\partial J}{\partial x} = e\mu_\mathrm{e}(E - E')\frac{\partial N_\mathrm{e}}{\partial x} + e\mu_\mathrm{e} N_\mathrm{e}\frac{\partial E}{\partial x} - e\mu_\mathrm{e} N_\mathrm{e}\frac{\partial E'}{\partial x} \tag{45}$$

The last term on the RHS is negligible compared to the others if the magnitude of the divergence of E' is less than the one of E:

$$\left|\frac{\partial E'}{\partial x}\right| \ll \left|\frac{\partial E}{\partial x}\right| \tag{46}$$

Also, at steady-state, the divergence of the current vanishes and the LHS of Eq. (45) becomes 0. Then, isolate the divergence of the electric field within Gauss's law Eq. (6) and substitute in Eq. (45) while setting N_i to zero

$$0 = e\mu_\mathrm{e}(E - E')\frac{\partial N_\mathrm{e}}{\partial x} - \frac{e^2}{\epsilon_0}\mu_\mathrm{e} N_\mathrm{e}^2 \tag{47}$$

Recall the current at the anode, Eq. (44), substitute in the latter, and isolate the electron number density. We thus obtain the boundary conditions at the solid-plasma surfaces where the electric field points away from the surface:

$$N_\mathrm{e} = \left(\frac{\epsilon_0 J}{e^2\mu_\mathrm{e}}\frac{\partial N_\mathrm{e}}{\partial x}\right)^{\frac{1}{3}} \quad \text{and} \quad N_\mathrm{i} = 0 \quad \text{for} \quad E_\eta > 0 \tag{48}$$

In deriving the latter from the standard anode boundary condition outlined in Eq. (42), three assumptions are made: (i) the current originating from a gradient of the electron mobility is assumed negligible compared to the other current components; (ii) the problem is assumed at steady-state; and (iii) the magnitude of the divergence of E' is assumed less than the magnitude of the divergence of E (see condition (46)). While the first two assumptions are generally well justified, it is not clear whether the third one would always be valid. For all test cases presented hereafter, it is verified that condition (46) is satisfied and that the anode boundary condition shown in Eq. (48) is valid. For other problem setups such as those involving multidimensional or magnetic field effects, it is cautioned that the anode sheath boundary condition shown above may need to be modified to yield the correct solution of Gauss's law at the surface.

We can combine Eq. (48) with Eq. (43) to obtain a general expression for the ion and electron densities at a surface boundary that is valid on anode, cathode, and dielectric boundaries. For instance, consider a boundary node denoted by the counter "i" and juxtaposed to an inner node at "$i+1$", and another inner node at "$i+2$". Then, the discretized equations used to update the charged species densities at the boundary node as a function of the properties at the nearby inner nodes can be written as:

$$\begin{aligned}(N_\mathrm{e})_i^{n+1} &= \alpha \times (N_\mathrm{e})_i + (1-\alpha) \\ &\times \begin{cases} \gamma \times (N_\mathrm{i})_{i+1} \times \left(\dfrac{\mu_\mathrm{i}}{\mu_\mathrm{e}}\right)_{i+1/2} & \text{if } E_\eta < 0 \\ \min\left((N_\mathrm{e})_{i+1},\ \max\left((N_\mathrm{i})_i^3\ ,\ \dfrac{\epsilon_0 J_{i+1/2}}{e^2(\mu_\mathrm{e})_{i+1/2}} \times \dfrac{(N_\mathrm{e})_{i+2} - (N_\mathrm{e})_{i+1}}{x_{i+2} - x_{i+1}}\right)^{1/3}\right) & \text{otherwise} \end{cases}\end{aligned} \tag{49}$$

$$(N_\mathrm{i})_i^{n+1} = \begin{cases} 0 & \text{if } E_\eta > 0 \\ (N_\mathrm{i})_{i+1} & \text{otherwise} \end{cases} \tag{50}$$

where $E_\eta = \text{minmod}\left(\phi_i - \phi_{i+1},\ \phi_{i+1} - \phi_{i+2}\right)/\Delta x$. To prevent convergence hangs, it is necessary to under-relax the electron density at the boundary by setting the relaxation factor α to a value higher than zero and lower than one. Through trial and error it is found that α should be given a value between 0.9 and 0.95 for optimal convergence. On the other hand, no relaxation is necessary when updating the ion density at the boundary. Because the relaxation factor vanishes from Eq. (49) when the solution is converged (that is, when $N_e^{n+1} \to N_e$), the value given to α does not affect the converged solution. This is the case not only for steady-state problems but also for time-accurate problems solved through a dual-time stepping approach.

The boundary nodes are updated after the ion and electron densities are updated but before the residual of the potential is determined. One iteration hence consists of, firstly, updating the ion and electron densities at the boundary nodes, then finding the residual of the potential equation, then updating the potential, then finding the residual of the ion and electron densities, and, lastly, updating the ion and electron densities at the inner nodes. Further, we note that the use of the electron density at the anode boundary shown in Eq. (48) is only necessary for the proposed governing equations. For the conventional governing equations, the electron number density at the anode is specified using the standard approach as outlined in Eq. (42).

8. Test Cases

Several test cases are now considered to assess the performance of the proposed governing equations over the conventional governing equations in solving sheaths. In all cases, the medium is a three-component air plasma including electrons, neutrals, and one type of positive ions. The electron and ion mobilities are as specified in Table 1 while the chemical reactions taking place within the plasma are listed in Table 2. In the chemical model used herein, the electron creation mechanisms are limited to Townsend ionization (*i.e.* electron impact ionization) and electron-beam ionization, while the sole electron loss mechanism consists of dissociative recombination. It is noted that the chemical model does not include the various electron gain and loss mechanisms in air due to excited species because such are not expected to play a significant role for the test cases considered. Further, we do not expect these additional chemical reactions to affect significantly the convergence characteristics and the resolution capabilities of the methods.

TABLE 1.
Ion and electron mobilities in air.[a]

Charged species	Mobility, $\text{m}^2 \cdot \text{V}^{-1} \cdot \text{s}^{-1}$	Reference
Air^+	$N^{-1} \cdot \min\left(8.32 \cdot 10^{22}/\sqrt{T},\ 2.13 \cdot 10^{12}/\sqrt{E^\star}\right)$	[30][b]
e^-	$N^{-1} \cdot 3.74 \cdot 10^{19} \cdot \exp\left(33.5/\sqrt{\ln(T_e)}\right)$	[31, Ch. 21][c]

[a] Notation and units: T_e is in Kelvin; T is in Kelvin; N is the total number density of the plasma in $1/\text{m}^3$; $E^\star$ is the reduced electric field ($E^\star = |E|/N$) in units of $\text{V}\cdot\text{m}^2$.

[b] The "air ion" mobility is obtained from the N_2^+ and O_2^+ ion mobilities assuming a N_2^+:O_2^+ ratio of 4:1.

[c] The expression approximates the data given in Chapter 21 of Ref. [31]; The equation can be used in the range 1000 K $\leq T_e \leq$ 57900 K with a relative error on the mobility not exceeding 20%. In the range 287 K $\leq T_e <$ 1000 K, the relative error is less than 30%.

TABLE 2.
Ionization and recombination reactions taking place within a 3-component ebeam-ionized air plasma.

No.	Reaction	Rate Coefficient[a]	References
1	$\text{e}^- + \text{Air} \to \text{Air}^+ + \text{e}^- + \text{e}^-$	$\exp(-0.0105031 \cdot \ln^2 E^\star - 2.40983 \cdot 10^{-75} \cdot \ln^{46} E^\star)$ cm^3/s	[32, 33, 31][b]
2	$\text{Air} \to \text{e}^- + \text{Air}^+$	$1.84 \cdot 10^{17} \cdot Q_b/N$ 1/s	[34]
3	$\text{e}^- + \text{Air}^+ \to \text{Air}$	$2.24 \cdot 10^{-7} \cdot (300/T_e)^{0.5} + 0.4 \cdot 10^{-7} \cdot (300/T_e)^{0.7}$ cm^3/s	[35][c]

[a] Notation and units: T_e is in Kelvin; T is in Kelvin; Q_b is the electron beam power deposited in W/m^3; N is the total number density of the plasma in $1/\text{m}^3$; $E^\star$ is the reduced electric field ($E^\star \equiv |E|/N$) in units of $\text{V}\cdot\text{m}^2$.

[b] The rate coefficient approximates the Townsend ionization rates given in [32] and in [33, p. 56] with the drift velocity taken from [31, Ch. 21]; The rate coefficient can be used in the range $3 \cdot 10^{-20} \leq E^\star \leq 240 \cdot 10^{-20}$ $\text{V} \cdot \text{m}^2$ with a relative error on the ionization rate not exceeding 20%.

[c] The rate coefficient approximates the dissociative recombination reactions $\text{e}^- + N_2^+ \to \text{N} + \text{N}$ and $\text{e}^- + O_2^+ \to \text{O} + \text{O}$ assuming a N_2^+:O_2^+ ratio of 4:1.

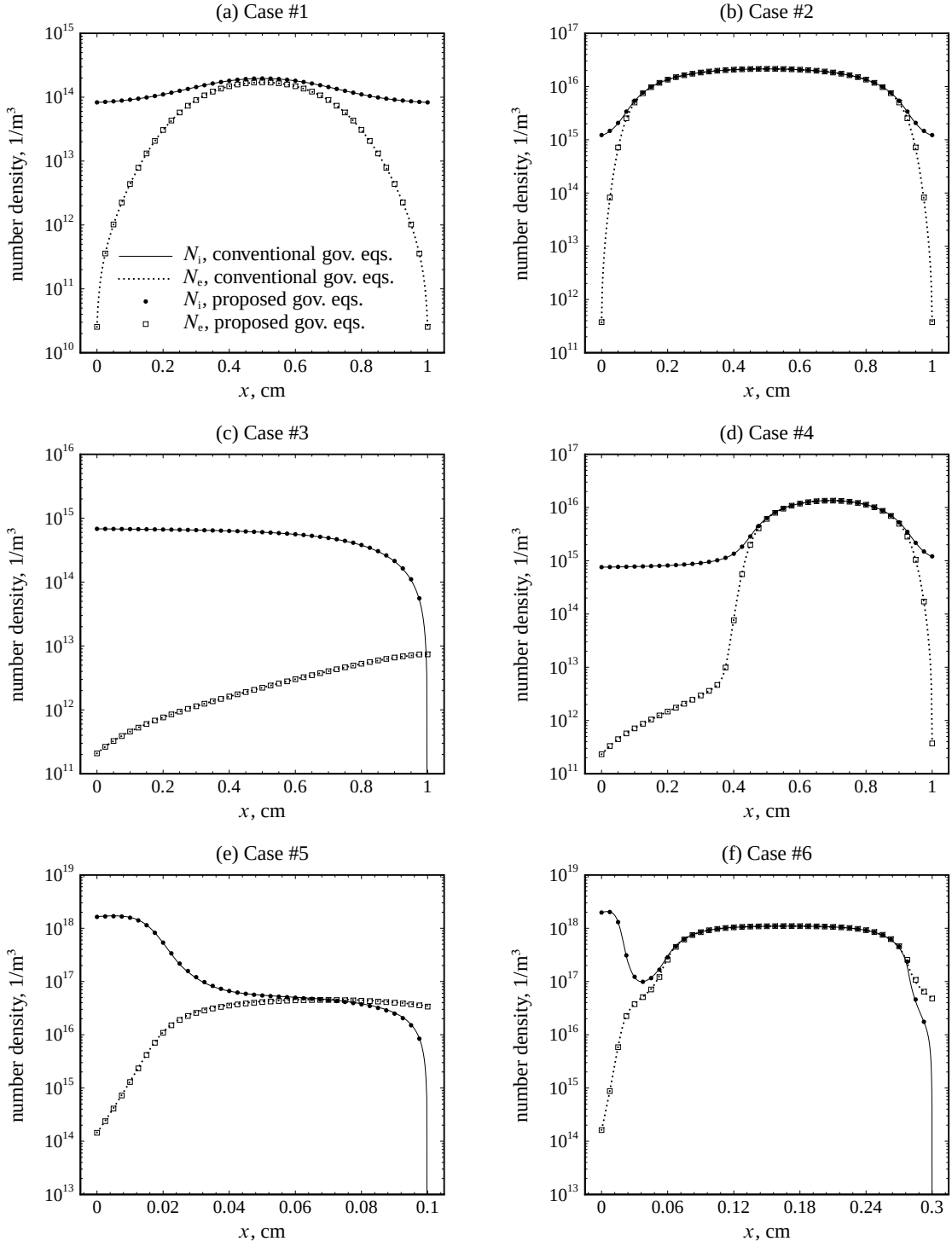

FIGURE 1. Electron and ion density at steady-state obtained with the conventional governing equations and the proposed governing equations in ambipolar form. For the proposed governing equations, 1 in every 10 nodes is shown for cases #1 to #5 while 1 in every 40 nodes is shown for case #6. The grid is composed of 401 equally-spaced nodes for all cases except for case #6 where it is composed of 1601 equally-spaced nodes.

As listed in Table 3, six air plasma test cases are considered in which the air is ionized with electron beams. The first two cases consist of a current-free plasma enclosed by dielectrics while the other four cases consist of a plasma located between two electrodes. For all cases involving cathode sheaths, steady state solutions obtained with the numerical method presented herein have been verified to yield a current density, voltage drop, and sheath thickness in accordance to those given by the one-dimensional cathode sheath theory outlined in [33, p. 180].

The ion and electron densities at steady-state obtained using the proposed method can be seen in Fig. 1 to be essentially identical to those obtained using the conventional approach. This is not particularly surprising. After all, both sets of governing equations are obtained from the same physical model, and they should yield the same solution as long as the grid is refined sufficiently and as long as the assumptions made in deriving the anode boundary condition remain valid. Indeed, it is recalled that the boundary conditions associated with the proposed method differ from the conventional approach when an anode sheath is present. Therefore, the fact that the present method results in essentially the same solution as the conventional approach in the presence of an anode sheath (as in test cases #5 and #6) validates the boundary conditions outlined in Section 7, at least for the one-dimensional steady-state problems here considered.

While the proposed governing equations yield essentially the same solution as the conventional governing equations, they are considerably less stiff and can be integrated using much higher pseudotime steps. For instance, in Table 4, we list the optimal relaxation parameters that give fastest convergence to steady-state. The conventional governing equations are so stiff that the CFL must be set to a value less than one for most test cases. Should the CFL number be set to a higher value, the solution would diverge towards aphysical states. The proposed governing equations, on the other hand, do not exhibit such stiffness and permit the use of a CFL number that is typically one thousand times greater. A higher CFL number entails a higher pseudotime step, and this is turn leads to much faster convergence to steady-state. In fact, as can be seen from Table 5, the use of the proposed set of equations results in a remarkable one-thousand-fold (or more) reduction in the number of iterations necessary to obtain steady state for several of the test cases.

We emphasize that the observed stiffness of the conventional sheath governing equations when solved with a block-implicit pseudotime relaxation procedure is not due to the disparate physical time scales. This is well demonstrated through the numerical results: when modeling sheaths involving quasi-neutral regions, the proposed set of equations does not exhibit considerable stiffness (the time step is not restricted substantially), while the conventional set of equations exhibits significant stiffness (the time step size is subject to severe restrictions), despite both sets of equations representing the same physical model and hence having the same disparate physical time scales. Obviously, the stiffness associated with the conventional sheath governing equations does not originate from the physical time scales but rather originates from the way the system of equations is formulated. Specifically, the stiffness of the conventional governing equations is here attributed to the electric field being obtained from Gauss's law rather than from Ohm's law, and from Gauss's law entailing severe convergence difficulties. Obtaining the potential from Gauss's law leads to a significant stiffness of the system of equations because of its dependence on the *difference* between the ion and electron densities:

$$-\epsilon_0 \nabla^2 \phi = e(N_\mathrm{i} - N_\mathrm{e}) \tag{51}$$

The difference between the electron and ion number densities is a quantity that is subject to considerable numerical error when the plasma is in the quasi-neutral state. This can be seen through the relative error on the difference between the ion and electron

TABLE 3.
Problem setup for the various test cases.[a]

Case	Description	Bulk properties				Boundary conditions		Initial conditions	
		L, cm	P, bar	N, 1/m^3	Q_b, W/m^3	$\phi_{x=0}$, V	$\phi_{x=L}$, V	N_i, 1/m^3	N_e, 1/m^3
#1	Dielectric sheaths	1	0.1	$2.414 \cdot 10^{24}$	10^0	0	0	10^{10}	10^{10}
#2	Dielectric sheaths	1	0.1	$2.414 \cdot 10^{24}$	10^2	0	0	10^{10}	10^{10}
#3	Dark discharge	1	0.1	$2.414 \cdot 10^{24}$	10^2	0	800	10^{10}	10^{10}
#4	Cathode sheath (low J)	1	0.1	$2.414 \cdot 10^{24}$	10^2	0	200	10^{10}	10^{10}
#5	Cathode sheath (high J)	0.1	0.1	$2.414 \cdot 10^{24}$	10^0	0	800	10^{16}	10^{16}
#6	Glow discharge	0.3	0.1	$2.414 \cdot 10^{24}$	$2 \cdot 10^5$	0	800	10^{16}	10^{16}

[a] In all cases, the secondary emission coefficient γ is set to 0.1, the electron temperature T_e is set to 20,000 K, the ion temperature T_i is set to 300 K, and the initial potential ϕ is set to 0 V.

TABLE 4.
Optimal relaxation parameters that yield fastest convergence to steady-state[a].

Case	Optimal relaxation parameters					
	Conventional governing equations			Proposed governing equations		
	CFL	L_c, m	α	CFL	L_c, m	α
#1	10.	1000	0.	500	1000	0.9
#2	0.02	1000	0.	250	1000	0.9
#3	500.	1000	0.	500	1000	0.991
#4	0.04	1000	0.95	500	1000	0.9
#5	0.2	1000	0.	50	1000	0.9
#6	0.005	1000	0.	10	1000	0.9

[a] A 100-node grid is used for cases #1 to #5 and a 200-node grid is used for case #6.

TABLE 5.
Comparison of the proposed governing equations to the conventional governing equations on the basis of number of iterations needed to reach steady-state[a,b,c].

Governing equations	Number of iterations needed to reach steady-state					
	Case #1	Case #2	Case #3	Case #4	Case #5	Case #6
Conventional	4,701	1,934,000	25	947,000	3,117	1,380,000
Proposed (ambipolar form)	171	203	2,294	196	1,950	6,444

[a] For cases 1-4, steady-state is reached when the maximum residual of the ion and electron densities falls below $10^{11}/\mathrm{m}^3\mathrm{s}$. For cases 5 and 6, steady-state is reached when the maximum residual of the ion and electron densities falls below $10^{16}/\mathrm{m}^3\mathrm{s}$.

[b] For cases #1 to #5, the grid is composed of 100 equally-spaced nodes. For case #6, the grid is composed of 200 equally-spaced nodes.

[c] The CFL number, the relaxation factor α, and the characteristic length scale L_c are chosen such as to yield optimal convergence rates (see Table 4).

densities, which can be shown to correspond to:

$$\mathcal{E}(N_i - N_e) = \frac{N_i \mathcal{E}(N_i) + N_e \mathcal{E}(N_e)}{|N_i - N_e|} \tag{52}$$

where the function $\mathcal{E}()$ here denotes the relative error of a certain quantity. For instance, consider a quasi-neutral plasma for which the ion density is within 0.1% of the electron density. Equation (52) yields an error on the difference between the ion and electron densities a thousand times greater than the error on either the ion number density or the electron number density. Because of such an error amplification within the solution of Gauss's law, the numerical error on the electron and ion densities must be kept to a minimum as the solution progresses in pseudotime. Thus, large pseudotime steps can not be used when solving either the ion or electron transport equations. Such a restriction on the pseudotime step size could be bypassed through the use of an implicit relaxation scheme should the system of conservation laws be linear. However, when the system of conservation laws is non-linear (as is the case herein), an implicit relaxation scheme would not prevent the error amplification through the solution of the potential obtained from Gauss's law and would hence be subject to more or less the same pseudotime step restrictions as an explicit scheme.

Further, we underscore that we are not solving here a set of uncoupled equations, but rather we are here solving a *system* of equations (*i.e.* a set of equations that are coupled to each other). In fact, it is the strong coupling between Gauss's law and the electron and ion conservation equations that is at the origin of the stiffness when the plasma is in the quasi-neutral state: the small errors necessarily associated with the update of the ion or electron densities become amplified by the potential equation based on Gauss's law, resulting in a large error in the potential (and hence the electric field) at the next iteration, which itself leads to a large error on the electron and ion densities at the following iteration because the latter depend on the electric field. This quickly leads to divergence towards aphysical states unless extremely small time steps are used to integrate the charged species equations.

If the slow convergence of the conventional governing equations is in fact due to the error amplification within the potential

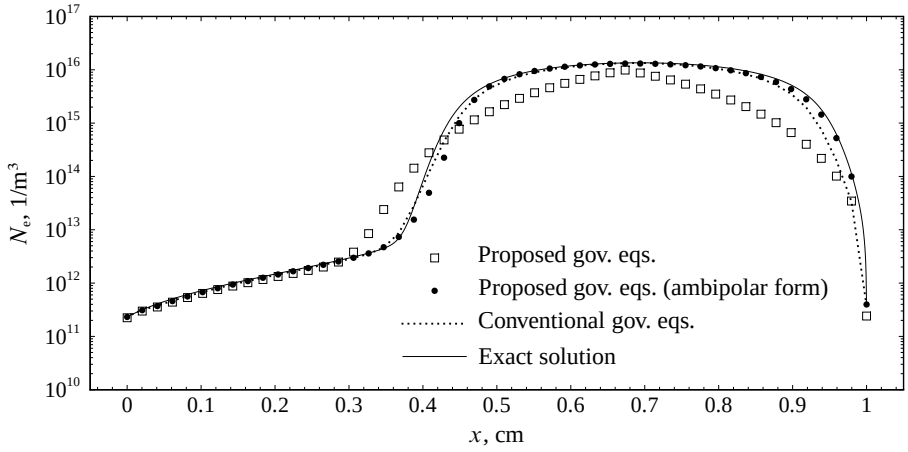

FIGURE 2. Comparison between the proposed governing equations, the proposed governing equations in ambipolar form, and the conventional governing equations on the basis of electron number density for test case #4 using a 50-node grid. The "exact" solution is obtained using the conventional governing equations and a 1600-node grid.

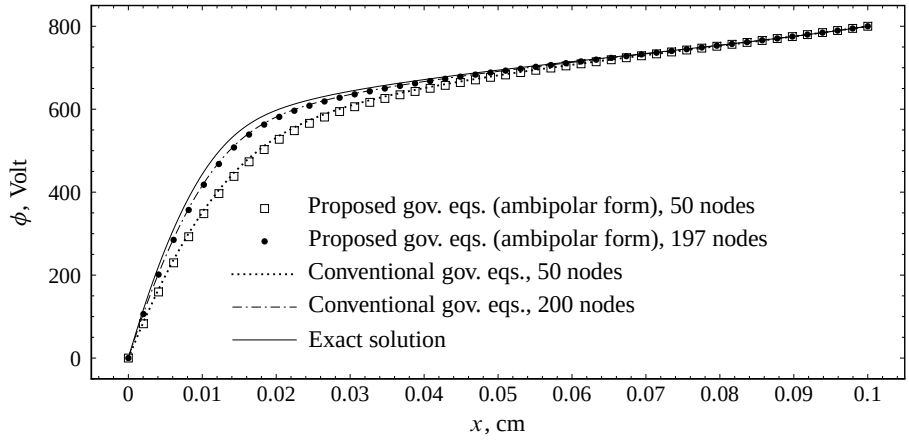

FIGURE 3. Impact of the grid size on the potential contours for test case #5. For the proposed governing equations using a 197-node mesh, one in every 4 nodes is shown. The "exact" solution is obtained using the conventional governing equations and a 3200-node grid.

equation obtained from Gauss's law, we would expect the conventional governing equations to restrict the CFL number to very small values when solving plasmas that include quasi-neutral regions. We would also expect the restrictions on the CFL to be relieved when the plasma does not include regions that approach the quasi-neutral state. As can be seen from Tables 4 and 5, this is precisely the behavior exhibited by the conventional governing equations. When solving plasmas that do not include quasi-neutral regions (test cases #1, #3 and #5), relatively high CFL numbers can be specified and this leads to convergence to steady-state in less than a few thousand iterations. When solving plasmas that do include a quasi-neutral region (test cases #2, #4, and #6), it is necessary to reduce the CFL to much lower values. This in turn leads to very slow convergence to steady-state in one million iterations or more.

It may be argued that the convergence acceleration gains of the present method over the conventional approach are obtained at the expense of accuracy. Such is verified not to be the case at least when the proposed governing equations are written in ambipolar form. In fact, a comparison between the different types of governing equations (see Figs. 2, 3, and 4) reveals that the proposed set of equations in ambipolar form yield an electron density, potential, and current more or less as close to the exact solution as the conventional set of equations. Such is corroborated by Tables 6 and 7 in which an assessment of the relative error on the ion density and the potential is provided for several meshes: in all cases, no significant difference in resolution between the present method and the conventional approach is apparent. This is verified to be the case within cathode sheaths,

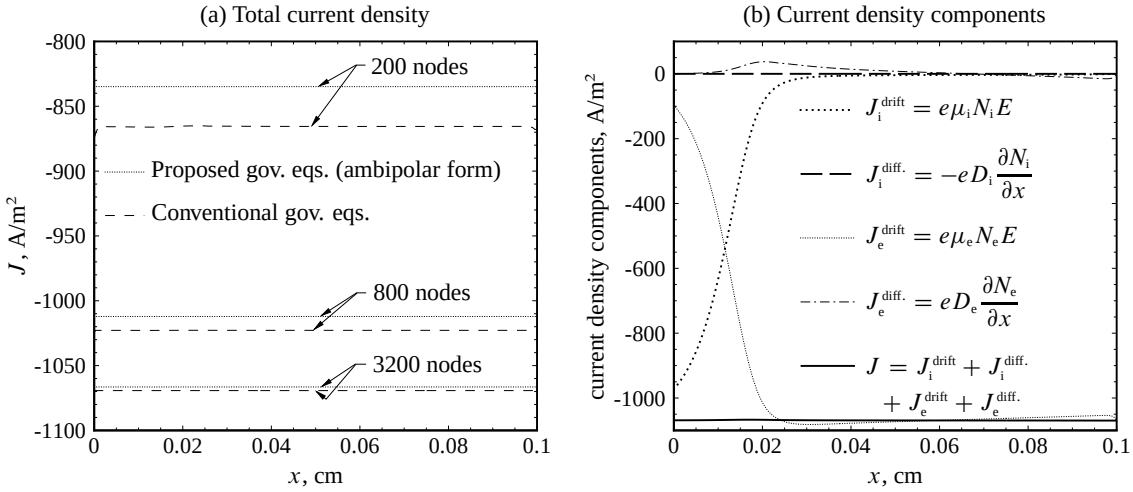

FIGURE 4. Total current density and current density components for test case #5 at steady-state: (a) comparison between the proposed governing equations in ambipolar form and the conventional governing equations on the basis of total current density for various grids, and (b) current density components obtained using the conventional governing equations and a 3200-node grid – see definition of the current density, Eq. (12).

TABLE 6.
Relative error assessment in solving test case #4 at steady-state.[a,b]

Governing equations	Average relative error					
	$\frac{1}{LN_{ref}}\int_0^L \lvert N_i - (N_i)_{exact}\rvert \, dx$			$\frac{1}{L\phi_{ref}}\int_0^L \lvert \phi - \phi_{exact}\rvert \, dx$		
	25 nodes	100 nodes	400 nodes	25 nodes	100 nodes	400 nodes
Proposed	43.3%	12.3%	1.9%	1.26%	0.52%	0.049%
Proposed (ambipolar form)	6.3%	1.4%	0.25%	0.89%	0.18%	0.033%
Conventional	11.3%	1.6%	0.13%	1.36%	0.19%	0.015%

[a] The "exact" solution is obtained using the conventional governing equations on a grid composed of 1600 equally-spaced nodes.
[b] The domain length is set to 1 cm, the reference ion number density N_{ref} is set to $10^{16}/m^3$, and the reference potential ϕ_{ref} is set to 400 V.

anode sheaths, dielectric sheaths, and within quasi-neutral regions.

Compared to the conventional set of equations, the proposed governing equations are significantly easier to integrate because they allow the use of much higher CFL number. As is shown in Table 4, the CFL number can be raised to values in excess of 100 when using the proposed method. This in turn leads to a substantial reduction in the number of iterations to reach steady-state. However, it is unlikely that such high CFL numbers can be specified when the electron and ion conservation equations are integrated in coupled form with the neutrals mass, momentum, and energy transport equations. This is due to the fact that non-linear stability restrictions generally prevent the CFL number to be raised to values significantly more than 1, even when using an implicit pseudotime stepping method. There are some flow regimes, however, for which this non-linear stability restriction does not apply, such as when the Mach number is sufficiently low that shocks are either not present or have a relatively low pressure ratio, or when the diffusion derivatives predominate over the convection derivatives. Actually, it turns out that sheaths are expected to be located in such flow regions. Indeed, because sheaths occur near surfaces where boundary layers are present, and because the sheath thickness is typically much less than the boundary layer thickness, the flow regions where the sheath will be located are expected to be such that the neutral gas is diffusion-dominated and has a low Mach number. It follows that, while we do not expect to be able to raise the CFL to values exceeding 100 when solving more intricate problems such as compressible flows studded with high-strength shocks, we expect to be able to raise the CFL number to values well exceeding 1 in the flow regions in which the sheaths are located.

Because it is likely that the CFL number may need to be reduced significantly from the values used herein when solving more complex problems, it is important to determine the impact that a change in the CFL number has on the convergence

TABLE 7.
Relative error assessment in solving test case #5 at steady-state.[a,b]

Governing equations	Average relative error					
	$\frac{1}{LN_{\text{ref}}}\int_0^L \lvert N_\text{i} - (N_\text{i})_{\text{exact}}\rvert \,\text{d}x$			$\frac{1}{L\phi_{\text{ref}}}\int_0^L \lvert \phi - \phi_{\text{exact}}\rvert \,\text{d}x$		
	50 nodes	200 nodes	800 nodes	50 nodes	200 nodes	800 nodes
Proposed	15%	5.7%	1.4%	7.2%	1.9%	0.43%
Proposed (ambipolar form)	15%	5.7%	1.4%	7.2%	1.9%	0.43%
Conventional	14%	4.8%	1.1%	6.4%	1.7%	0.34%

[a] The "exact" solution is obtained using the conventional governing equations on a grid composed of 3200 equally-spaced nodes.

[b] The domain length L is set to 0.1 cm, the reference ion number density N_{ref} is set to $10^{18}/\text{m}^3$, and the reference potential ϕ_{ref} is set to 400 V.

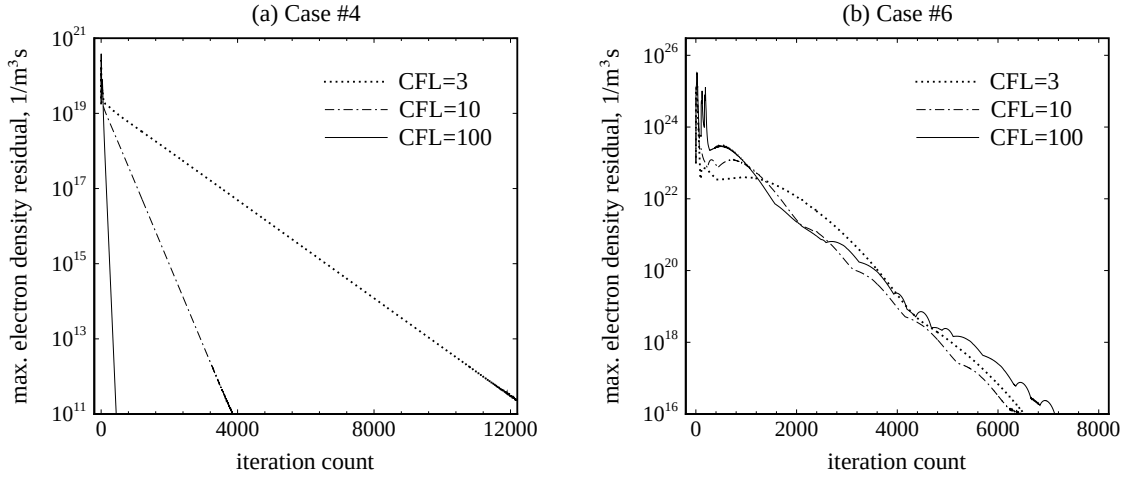

FIGURE 5. Impact of the CFL number on the convergence rate when using the proposed governing equations in ambipolar form. A 100-node grid is used for case #4 and a 200-node grid is used for case #6. The relaxation parameters α and L_c are as specified in Table 4.

characteristics of the present method, and to determine if the latter would still yield an advantage over the conventional approach in the worst case scenario (*i.e.*, when the CFL is as low as 1). Interestingly, the CFL number is seen to have a small impact on the convergence rate when solving a high-current glow discharge typical of plasma aerodynamic applications (see Fig. 5b). On the other hand, the CFL number is seen to have a more pronounced impact on the convergence rate of the electron density residual when solving low-current cathode sheaths juxtaposed to a quasi-neutral region (see Fig. 5a). Nonetheless, for both cases, it is verified that the proposed governing equations are advantaged over the conventional set of equations even for the lowest CFL number considered: throughout the range $3 \leq \text{CFL} \leq 500$, the present method is seen to yield a reduction in computing effort of at least one-hundred-fold and as much as ten-thousand-fold.

We now proceed to demonstrate through some test cases that the set of governing equations proposed herein yields benefits over the conventional set of equations not only for steady-state problems, but also for time-accurate problems. A time-accurate solution is here obtained through dual-time stepping. Dual-time stepping consists of adding the time derivative to the residual and of performing pseudotime iterations at each time level until the residual falls below a certain user-defined convergence threshold. A dual-time stepping approach is advantaged over a single-step implicit time stepping strategy by guaranteeing that the discrete equations are converged at each time level, hence increasing significantly the accuracy of the solution. As well, a dual-time stepping approach is advantaged over an explicit time stepping method by permitting the use of much higher time steps. This is particularly beneficial when solving sheath problems where large differences in time scales exist between the chemical reactions, diffusion, and convection phenomena. When using a time accurate dual-time stepping algorithm to solve a glow discharge with a quasi-neutral positive column, the proposed set of equations results in a reduction in computing effort of 30–100 times compared to the conventional set (see Table 8). This significant gain in convergence acceleration is obtained with

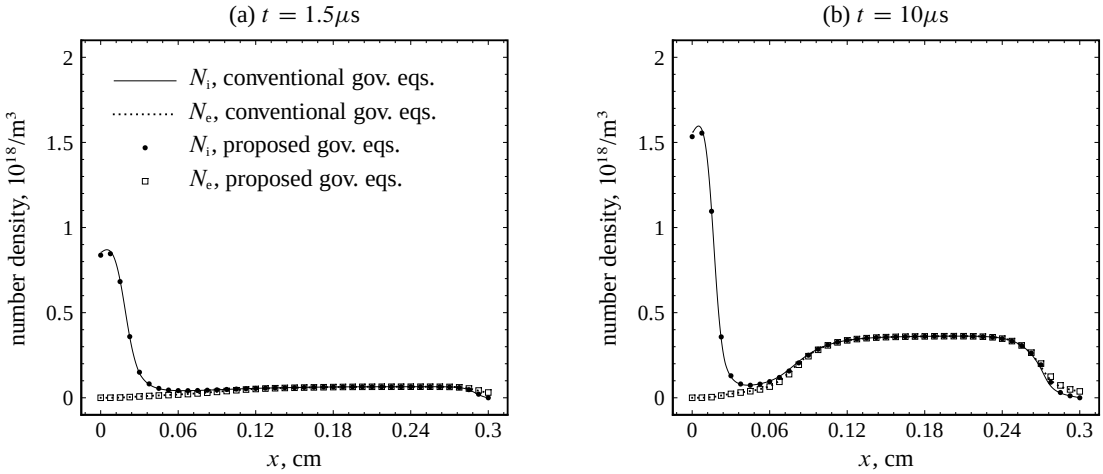

FIGURE 6. Time accurate profiles of the ion and electron densities for case #6 obtained with the conventional governing equations and the proposed governing equations in ambipolar form. For both sets of governing equations, the grid is composed of 801 equally-spaced nodes and the time step is set to 0.5 microsecond. For the proposed governing equations, 1 in every 20 nodes is shown.

TABLE 8.
Average number of iterations per time level when solving case #6 using a time accurate algorithm [a,b,c].

Governing equations	Average number of iterations per time level			
	200 nodes	400 nodes	800 nodes	1600 nodes
Conventional	36,000	85,800	183,000	357,200
Proposed (ambipolar form)	1,003	1,585	2,086	3,179

[a] At each time level, the solution is considered converged when the maximum residual of the ion and electron densities falls below $10^{19}/m^3s$.
[b] The CFL number, the relaxation factor α, and the characteristic length scale L_c are chosen such as to yield optimal convergence rates (see Table 4).
[c] The average is taken over the first 20 time levels, with the time step size set equal to 0.5 microsecond.

essentially no penalty in resolution. In fact, the electron and density contours obtained with each approach show no discernible difference as long as the mesh is refined sufficiently to yield a grid-independent solution (see Fig. 6). On coarser meshes, it is verified that, similarly to steady-state problems, the average relative error on the potential and the electron and ion densities is essentially unaffected when the proposed governing equations are solved instead of the conventional governing equations.

9. Conclusions

To date, the numerical simulation of plasma sheaths using macroscopic-scale transport equations has involved the coupling of the electric field potential equation obtained through Gauss's law to the electron and ion transport equations obtained through the drift-diffusion model. When discretized using finite difference stencils, this set of equations (referred herein as the "conventional governing equations") is particularly stiff and typically requires hundreds of thousands of iterations to reach convergence whenever a quasi-neutral region forms adjacent to the sheath. This is attributed to the potential equation obtained from Gauss's law amplifying in quasi-neutral regions the numerical error associated with the electron or ion densities. Because of such an error amplification within the solution of Gauss's law, the numerical error on the charged species densities must be kept to a minimum as the solution progresses in pseudotime. Thus, large pseudotime steps can not be used when solving either the ion or electron transport equations, and this in turn leads to an excessive number of iterations to reach convergence.

A new set of sheath governing equations is presented here that is such that the electric field is obtained from Ohm's law rather than from Gauss's law. To ensure that Gauss's law is satisfied, some source terms are added to the ion conservation equation. In doing so, the potential equation is not strongly dependent on the difference between the ion and electron number densities, and this relieves the stiffness associated with its integration. The proposed governing equations are found through several test cases

to result in a remarkable improvement in computational efficiency compared to the conventional set of equations. The number of iterations needed to reach convergence is typically reduced one-hundred-fold to ten-thousand-fold whenever a quasi-neutral region is present within the plasma. This is confirmed to be the case not only for steady-state but also for time-accurate solutions of sheaths.

What makes the approach proposed herein particularly appealing is that it does not sacrifice accuracy in favor of convergence acceleration. For all test cases here considered, including steady-state and time-accurate simulations of dielectric sheaths, cathode sheaths, anode sheaths, dark discharges, and glow discharges, the present set of equations results in a solution that is essentially identical to the one obtained from the conventional set as long as the mesh is refined sufficiently. When the mesh is coarse and the numerical error significant, the resolution exhibited by both approaches is more-or-less the same: independently of the mesh size, the proposed governing equations are found to yield a numerical error on the potential and the charged species densities that does not exceed significantly the one exhibited by the conventional governing equations. Yet another appeal of the present approach is that it can be used in conjunction with any relaxation technique (such as block-implicit pseudotime relaxation, JFNK, LUSGS, multigrid, *etc.*). That is, the use of the proposed governing equations is expected to yield considerably faster convergence also when using alternate relaxation techniques, not only when using the block-implicit pseudotime relaxation technique as done herein.

It is cautioned that the method presented in this paper does have one disadvantage over the conventional approach. Specifically, because the potential equation is obtained from Ohm's law and not from Gauss's law, it is necessary to reformulate the boundary conditions at the anode in order to ensure that Gauss's law is satisfied within the anode sheath. The reformulated anode boundary condition is disadvantaged over the standard approach by requiring a more substantial relaxation of the electron density at the boundary. While this is generally not problematic, it does lead to some relatively slow convergence when simulating dark discharges devoid of a quasi-neutral region. Furthermore, we note that while the newly formulated anode boundary condition has been verified to yield the same solution as the standard approach for all test cases considered, it is not clear whether it would remain valid in more intricate problem setups (such as when the sheath is multidimensional, when the sheath is affected by the magnetic field, or when the plasma has several types of ion species). Further investigation is hence necessary to extend the boundary conditions at the anode, as well as the governing equations proposed herein, to multicomponent, multidimensional, and magnetized plasmas.

Acknowledgment

This research was supported by the Basic Science Research Program through the National Research Foundation of Korea (NRF) funded by the Ministry of Education, Science and Technology (Grant #2010-0023957).

References

[1] WAN, T., CANDLER, G. V., MACHERET, S. O., AND SHNEIDER, M. N., "Three-Dimensional Simulation of the Electric Field and Magnetohydrodynamic Power Generation During Reentry," *AIAA Journal*, Vol. 47, No. 6, 2009, pp. 1327.

[2] PARENT, B., MACHERET, S., SHNEIDER, M., AND HARADA, N., "Numerical Study of an Electron-Beam-Confined Faraday Accelerator," *Journal of Propulsion and Power*, Vol. 23, No. 5, 2007, pp. 1023–1032.

[3] HUANG, P. G., SHANG, J. S., AND STANFIELD, S. A., "Periodic Electrodynamic Field of Dielectric Barrier Discharge," *AIAA Journal*, Vol. 49, No. 1, 2011, pp. 119.

[4] SHANG, J. S. AND SURZHIKOV, S. T., "Magnetoaerodynamic Actuator for Hypersonic Flow Control," *AIAA Journal*, Vol. 43, No. 8, 2005, pp. 1633.

[5] LIKHANSKII, A. V., SHNEIDER, M. N., MACHERET, S. O., AND MILES, R. B., "Modeling of Dielectric Barrier Discharge Plasma Actuators Driven by Repetitive Nanosecond Pulses," *Physics of Plasmas*, Vol. 14, No. 7, 2007.

[6] PARKER, S. E., PROCASSINI, R. J., AND BIRDSALL, C. K., "A Suitable Boundary Condition for Bounded Plasma Simulation without Sheath Resolution," *Journal of Computational Physics*, Vol. 104, 1993, pp. 41–49.

[7] LIU, J.-Y., WANG, Z.-X., AND WANG, X., "Sheath Criterion for a Collisional Sheath," *Physics of Plasmas*, Vol. 10, No. 7, 2003, pp. 3032–3034.

[8] VASENKOV, A. V. AND D., S. B., "Numerical Study of a Direct Current Plasma Sheath Based on Kinetic Theory," *Physics of Plasmas*, Vol. 9, No. 2, 2002, pp. 691–700.

[9] SORIA-HYO, C., PONTIGA, F., AND CASTELLANOS, A., "A PIC Based Procedure for the Integration of Multiple Time Scale Problems in Gas Discharge Physics," *Journal of Computational Physics*, Vol. 228, 2009, pp. 1017–1029.

[10] GRAVES, D. B. AND JENSEN, K. F., "A Continuum Model of DC and RF Discharges," *IEEE Transactions on Plasma Science*, Vol. PS-14, No. 2, 1986, pp. 78–91.

[11] SCHMITT, W., KOHLER, W. E., AND RUDER, H., "A One-Dimensional Model of DC Glow Discharges," *Journal of Applied Physics*, Vol. 71, No. 12, 1992, pp. 5783–5791.

[12] ROY, S., PANDLEY, B. P., POGGIE, J., AND GAITONDE, D. V., "Modeling Low Pressure Collisional Plasma Sheath with Space-Charge Effect," *Physics of Plasmas*, Vol. 10, No. 6, 2002, pp. 2578–2585.

[13] MACHERET, S. O., SHNEIDER, M. N., AND MILES, R. B., "Modeling of Air Plasma Generation by Repetitive High-Voltage Nanosecond Pulses," *IEEE Transactions on Plasma Science*, Vol. 30, No. 3, 2002, pp. 1301–1314.

[14] SURZHIKOV, S. T. AND SHANG, J. S., "Two-Component Plasma Model for Two-Dimensional Glow Discharge in Magnetic Field," *Journal of Computational Physics*, Vol. 199, 2004, pp. 437–464.

[15] POGGIE, J., "Numerical Simulation of Direct Current Glow Discharges for High-Speed Flow Control," *Journal of Propulsion and Power*, Vol. 24, No. 5, 2008, pp. 916–922.

[16] ZHU, P., LOWKE, J. J., AND MORROW, R., "A Unified Theory of Free Burning Arcs, Cathode Sheaths and Cathodes," *Journal of Physics D: Applied Physics*, Vol. 25, 1992, pp. 1221–1230.

[17] MORROW, R. AND LOWKE, J. J., "A One-Dimensional Theory for the Electrode Sheaths of Electric Arcs," *Journal of Physics D: Applied Physics*, Vol. 26, 1993, pp. 634–642.

[18] LOWKE, J. J., MORROW, R., AND HAIDAR, J., "A Simplified Unified Theory of Arcs and their Electrodes," *Journal of Physics D: Applied Physics*, Vol. 30, 1997, pp. 2033–2042.

[19] LAMBERT, J. D., *Numerical Methods for Ordinary Differential Systems*, John Wiley and Sons, New-York, NY, 1991.

[20] PARENT, B., MACHERET, S. O., AND SHNEIDER, M. N., "Ambipolar Diffusion and Drift in Computational Weakly-Ionized Plasmadynamics," *Journal of Computational Physics*, Vol. 230, No. 22, 2011, pp. 8010–8027.

[21] CHOE, H.-H., YOON, N. S., KIM, S. S., AND CHOI, D.-I., "A New Unconditionally Stable Algorithm for Steady-State Fluid Simulation of High Density Plasma Discharge," *Journal of Computational Physics*, Vol. 170, 2001, pp. 550–561.

[22] CRISPEL, P., DEGOND, P., AND VIGNAL, M.-H., "An asymptotic preserving scheme for the two-fluid Euler-Poisson model in the quasineutral limit," *Journal of Computational Physics*, Vol. 223, 2007, pp. 208–234.

[23] PARENT, B., SHNEIDER, M. N., AND MACHERET, S. O., "Generalized Ohm's Law and Potential Equation in Computational Weakly-Ionized Plasmadynamics," *Journal of Computational Physics*, Vol. 230, No. 4, 2011, pp. 1439–1453.

[24] ROZHANSKY, V. A. AND TSENDIN, L. D., *Transport Phenomena in Partially Ionized Plasma*, Taylor and Francis, New-York, NY, 2001.

[25] RAMSHAW, J. D. AND CHANG, C. H., "Ambipolar Diffusion in Two-Temperature Multicomponent Plasmas," *Plasma Chemistry and Plasma Processing*, Vol. 13, No. 3, 1993, pp. 489–498.

[26] RAMSHAW, J. D. AND CHANG, C. H., "Multicomponent Diffusion in Two-Temperature Magnetohydrodynamics," *Physical Review E*, Vol. 53, No. 6, 1996, pp. 6382–6388.

[27] STEGER, J. L. AND WARMING, R. F., "Flux Vector Splitting of the Inviscid Gasdynamic Equations with Application to Finite-Difference Methods," *Journal of Computational Physics*, Vol. 40, 1981, pp. 263–293.

[28] VAN LEER, B., "Towards the Ultimate Conservation Scheme II. Monotonicity and Conservation Combined in a Second-Order Scheme," *Journal of Computational Physics*, Vol. 14, 1974, pp. 361–370.

[29] RAIZER, Y. P. AND SURZHIKOV, S. T., "Charge Diffusion Along a Current and an Effective Method of Eliminating Computational Diffusion for Glow Discharges," *High Temperature*, Vol. 28, No. 3, 1990, pp. 324–328.

[30] SINNOTT, G., GOLDEN, D. E., AND VARNEY, R. N., "Positive-Ion Mobilities in Dry Air," *Physical Review*, Vol. 170, No. 1, 1968, pp. 272–275.

[31] GRIGORIEV, I. S. AND MEILIKHOV, E. Z., *Handbook of Physical Quantities*, CRC, Boca Raton, Florida, 1997.

[32] MNATSAKANYAN, A. K. AND NAIDIS, G. V., "Processes of Formation and Decay of Charged Particles in Nitrogen-Oxygen Plasmas," *Khimiia Plazmy [Plasma Chemistry]*, edited by B. M. Smirnov, Vol. 14, Energoatomizdat, Moscow, Russia, 1987, pp. 227–255, in russian.

[33] RAIZER, Y. P., *Gas Discharge Physics*, Springer-Verlag, Berlin, Germany, 1991.

[34] PETERSON, L. R. AND GREEN, A. E. S., "The Relation Between Ionization Yields, Cross Sections, and Loss Functions," *Journal of Physics B: Atomic, Molecular and Optical Physics*, Vol. 1, No. 6, 1968, pp. 1131–1140.

[35] KOSSYI, A., KOSTINSKY, A. Y., MATVEYEV, A. A., AND SILAKOV, V. P., "Kinetic Scheme of the Non-Equilibrium Discharge in Nitrogen-Oxygen Mixtures," *Plasma Sources Science and Technology*, Vol. 1, 1992, pp. 207–220.